EEG Based Dynamic Functional Connectivity Analysis in Mental Workload Tasks With Different Types of Information

Kai Guan, *Graduate Student Member, IEEE*, Zhimin Zhang, Xiaoke Chai, Zhikang Tian, Tao Liu, and Haijun Niu, *Member, IEEE*

***Abstract*— The accurate evaluation of operators' mental workload in human-machine systems plays an important role in ensuring the correct execution of tasks and the safety of operators. However, the performance of cross-task mental workload evaluation based on physiological metrics remains unsatisfactory. To explore the changes in dynamic functional connectivity properties with varying mental workload in different tasks, four mental workload tasks with different types of information were designed and a newly proposed dynamic brain network analysis method based on EEG microstate was applied in this paper. Six microstate topographies labeled as Microstate A-F were obtained to describe the task-state EEG dynamics, which was highly consistent with previous studies. Dynamic brain network analysis revealed that 15 nodes and 68 pairs of connectivity from the Frontal-Parietal region were sensitive to mental workload in all four tasks, indicating that these nodal metrics had potential to effectively evaluate mental workload in the cross-task scenario. The characteristic path length of Microstate D brain network in both Theta and Alpha bands decreased whereas the global efficiency increased significantly when the mental workload became higher, suggesting that the cognitive control network of brain tended to have higher function integration property under high mental workload state. Furthermore, by using a SVM classifier, an averaged classification accuracy of 95.8% for within-task and 80.3% for cross-task mental workload discrimination were achieved. Results implies that it is feasible to evaluate the cross-task mental workload using the dynamic functional connectivity metrics under specific microstate, which provided a new insight for understanding the neural mechanism of mental workload with different types of information.**

***Index Terms*— Mental workload, different information types, EEG, microstate analysis, dynamic functional connectivity.**

I. Introduction

MENTAL workload (MWL) refers to the psychological stress felt by operators or the cognitive resources consumption while performing tasks [1], [2]. Excessive mental workload might affect operator's judgment and performance in human-machine interaction tasks such as manipulating airplanes or unmanned air vehicles, which posed threats to their safety [3]. The accurate evaluation of mental workload plays a significant role in ensuring the correct execution of tasks and the safety of operators. Frequently used methods of evaluating mental workload include subjective measurement (e.g., NASA-TLX, SWAT, etc. [4]), task performance measurement (e.g., response time, accuracy, etc.), and physiological measurement (e.g., EEG, ECG, etc. [5]–[7]). Compared with subjective measurement and task performance measurement, physiological measurement can objectively, continuously assess operator's mental workload without influencing the execution of task and therefore has attracted more attention from researchers.

Numerous researches indicated that different mental workload levels can be effectively distinguished by using physiological metrics in single task. However, when the same metrics were applied to the cross-task mental workload evaluation, it tended to end up with an unsatisfactory result with low accuracy. Metrics that can effectively assess mental workload in different tasks have not been proposed [8], [9].

Many studies attributed the cross-task problem to different information processing mechanisms of human brain while performing different tasks [9]–[11]. Specifically, different brain regions were involved when processing different types of information, and the activation patterns of them differed from each other, which leaded to the changes in physiological metrics differed [12]–[14]. Certain physiological metrics were often sensitive to tasks with a certain type of information,

Manuscript received October 21, 2021; revised February 6, 2022 and February 26, 2022; accepted March 1, 2022. Date of publication March 3, 2022; date of current version March 18, 2022. This work was supported in part by the State key Laboratory of Software Development Environment under Grant SKLSDE-2021ZX-08; in part by the Key Research and Development Project of Shanxi Province under Grant 201903D321167; and in part by the Open Research Fund from Beijing Advanced Innovation Center for Big Data-Based Precision Medicine, Beijing Tongren Hospital, Beihang University and Capital Medical University, under Grant BHTR-KFJJ-202008. *(Corresponding author: Haijun Niu.)*

This work involved human subjects or animals in its research. Approval of all ethical and experimental procedures and protocols was granted by the Beihang University Ethics Committee.

The authors are with the State Key Laboratory of Software Development Environment, and the Beijing Advanced Innovation Center for Biomedical Engineering, School of Biological Science and Medical Engineering, Beihang University, Beijing 100191, China (e-mail: guankaer@buaa.edu.cn; zhiminzhang@buaa.edu.cn; chaixiaoke@buaa.edu.cn; zk_tian@buaa.edu.cn; tao.liu@buaa.edu.cn; hjniu@buaa.edu.cn).

Digital Object Identifier 10.1109/TNSRE.2022.3156546

while these metrics cannot effectively characterize the change of mental workload in other tasks. There are various types of information in actual human-machine interaction tasks. The information that affects operator's mental workload levels mainly include verbal, images (or object) and spatial types. Clarifying the changes of physiological metrics with mental workload in different tasks and further selecting "task-independent" metrics that can evaluate mental workload effectively in all tasks might provide valuable references for establishing accurate and robust cross-task mental workload evaluation models [15], [16].

It was commonly accepted that EEG is the most sensitive physiological metric for its more direct reflection of the process of human brain compared with ECG, heart rate, eye movement, skin temperature, etc. Previous studies found that spectral power of the Theta and Alpha band of EEG can effectively reflect the change of operators' mental workload [17]–[20]. Gevin [17] and Popov [18] found that the power of Frontal Theta increased and Parietal Alpha decreased along with the increment of the task load in Verbal and Spatial N-Back tasks. Change of the EEG power in specific frequency bands mainly reflected the regional properties of the brain under workload. Considering that multiple brain regions were involved and these brain regions worked coordinatively while processing information, it would be beneficial to explore the interaction patterns of different brain regions in different tasks for the accurate evaluation of cross-task mental workload [21]–[23].

Recently, the functional connectivity based mental workload evaluation method has attracted the attention of researchers [24], [25]. It has been previously validated that the metrics of functional connectivity can be used to assess mental workload in single tasks (such as in Verbal N-Back task [21], Object working memory task [26], etc.). However, the traditional static functional connectivity analyses assumed that the statistic dependencies between brain regions kept constant when processing information, which neglected the time-varying property of brain activity [25], [27], [28].

To bridge this gap, a dynamic functional connectivity method with slide windows was proposed [29]. However, the selection of window size and slide step would directly influence the results. Meanwhile, a fix-size window cannot reflect the cognitive processing stage precisely [30]. The EEG microstates analysis considered that the brain activity remained quasi-stable for a short period (60 $\sim$ 120ms) while processing information and these quasi-stable states were thought to be closely related to specific cognitive processing stages (many studies regarded the microstates as the building blocks of consciousness) [31]–[33]. In the microstate analysis, EEG topography at each time point was assigned to one "Microstate" based on clustering methods. Compared with slide-window methods, microstates and their dynamic properties can characterize the cognitive stages of brain more precisely. Various studies implied that the dynamic properties of EEG microstates can effectively reflect the change of brain state when operators were performing tasks. Deolindo [34] found that the dynamic properties of microstates can be used to distinguish the situation awareness levels of helicopter pilots. Krylova's research showed that the microstate metrics were statistically correlated with the vigilance level of human [35]. Therefore, it is reasonable to believe that the topological characteristics of brain networks under specific microstates can reflect the mental workload of operators more precisely.

Considering all the above, it is expected to understand and solve the cross-task problem from a new insight by exploring how the dynamic functional connectivity properties change with mental workload when performing different tasks by using the dynamic brain network analysis and microstate analysis based on EEG. In this paper, four mental workload tasks with different information types (i.e., Verbal, Object, Spatial (Verbal) and Spatial (Object)) were designed. On the basis of the microstate analysis, dynamic functional connectivity networks under different microstates were constructed by calculating the Phase-Locking Value (PLV) between EEG channels. Statistical analysis was carried out to explore the changes of microstate metrics and brain network metrics with mental workload under different task conditions. At last, a Support Vector Machine (SVM) classifier was used to validate the effectiveness of the proposed method and the selected dynamic functional connectivity features in discriminating mental workload both in within-task and cross-task scenario.

II. Methods

A. Subjects

Sixteen right-handed, healthy subjects (8 males and 8 females, Age: 25.6 ± 2.4 years) participated in the study. None of the participants had histories of neurological diseases. All participants signed written informed consent and the study was approved by Beihang University Ethics Committee.

B. Experiment Protocol

The flowchart of the whole study was presented in Fig. 1. N-Back paradigm was used to carry out the experiment. Participants were instructed to judge if the information presented now is matched to the one presented previously. Four types of information were used in this study, namely Verbal, Object, Spatial (Verbal), and Spatial (Object), in which the verbal and object items were presented in different positions of a 3×3 matrix. In the Verbal and Object task, participants needed to judge if letters (or objects) were matched without considering their positions; and in the two spatial tasks, positions of the items (letters or objects) were the only information needed to be considered. Three task loads were set by manipulating the "N" from 1 to 3, which means there are 12 tasks in total. Participants performed the 12 tasks in a random sequence. A detailed illustration of the used N-Back tasks (Verbal and Spatial (Object)) can be seen in Fig. 2.

Taking the Verbal 2-Back task as an example, letters were presented on the screen sequentially every 2.5 seconds, each of them was displayed for 0.5 seconds and then disappeared. Participants should determine whether the present letter is the same as the letter two trials earlier. If so, "$\leftarrow$" should be pressed and conversely "$\rightarrow$". All participants needed to perform 40 trials in each task at each level of load, 50% of which were set as matching answers. Response time of

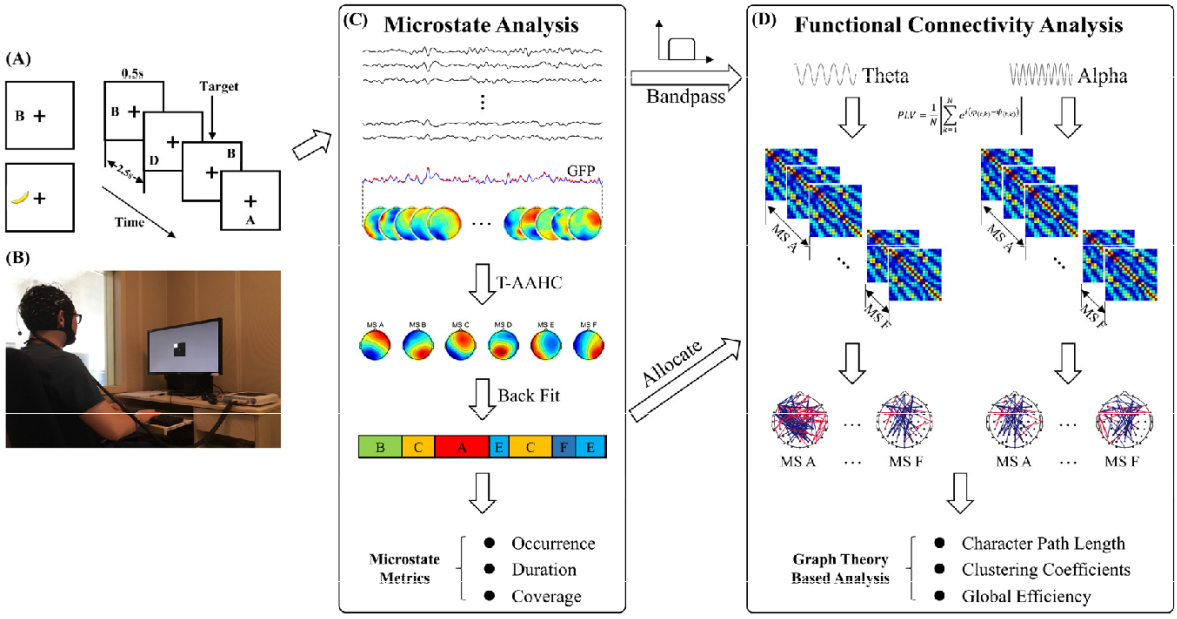

Fig. 1. Flowchart of the analysis framework. (A) The N-Back task paradigm. (B) The experiment setup. (C) Microstate analysis procedures. Step 1: Calculate EEG GFP of each trial in each task condition, Step 2: EEG data corresponding to the maxima of GFP were submitted into the T-AAHC clustering algorithm to get an individual-level microstate, the group-level microstates were obtained by a second time clustering, Step 3: Back fit and calculate the microstate metrics. (D) Dynamic functional connectivity analysis procedures. PLV was used to calculate the statistical dependencies between EEG channels in theta and alpha bands firstly, brain networks of specific microstate were obtained by average the functional connectivity with the same microstate allocated in (C), nodal and global metrics were calculated at last.

each trial was recorded during the experiments, accuracy of each task was calculated. After each task, NASA-TLX scale was required to be finished for subjective evaluation. Specifically, the NASA-TLX scale uses six dimensions (i.e., mental demand, physical demand, temporal demands, performance, effort, and frustration) to assess mental workload. Participants were asked to complete rating on each dimension (ranging from 0 to 100) and give weightings for each dimension to obtain a global score [4].

C. Data Acquisition and Pre-Processing

The experiments were carried out in a sound-shielded room. EEGs (60 channels, electrodes were placed according to 10–20 standard) were recorded at 1000Hz by using the NeuroScan system. The electrode impedances were kept below $10k\Omega$ during recording.

Only trials with successful responses were further analyzed in this study. Firstly, a bandpass filter (0.5-40Hz) was applied to eliminate direct components and noises with high frequencies. Eye blinks, vertical/horizontal EOGs, and EMGs were removed from the original EEGs by using the auto-recognition algorithm SASICA after resampling signals at 256Hz [36]. Data were segmented into epochs that started 500ms before stimulus onset and ended 2000ms after stimulus onset.

D. Microstate Analysis

Consistent microstate classes cannot be obtained by the prevalently used k-means clustering method since it is sensitive to the selection of clustering centers. Therefore, the Topographic Atomize & Agglomerate Hierarchical Clustering (T-AAHC) algorithm was used to carry out microstate analysis in this paper [37], [38]. The T-AAHC algorithm takes all the EEG topographies as original clusters at first and ends

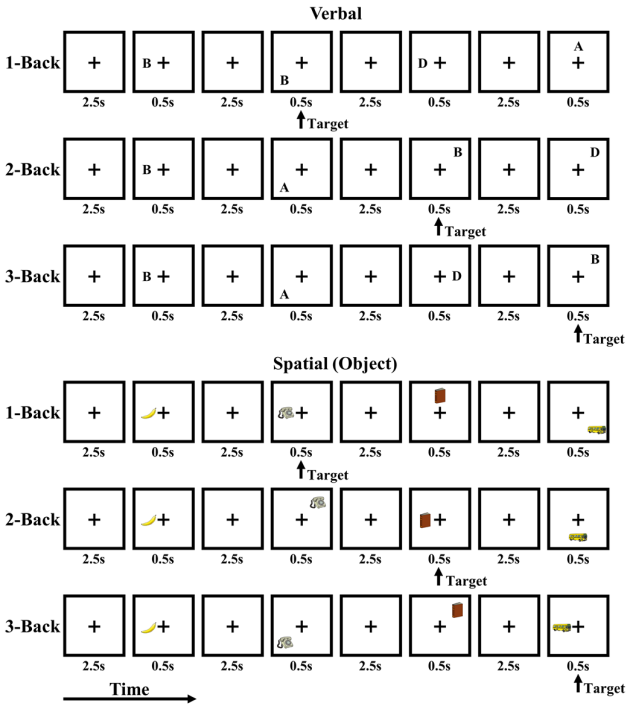

Fig. 2. Illustration of the N-Back paradigm. In the Verbal/Object task, participants need to determine whether the present letter/object is the same as the letter/object N trials earlier, and in the spatial tasks, only the location of the items should be considered.

with a limited number of clusters by removing the "worst" cluster and assigning each member of it to the clusters they are most similar to in each iteration. The specific procedure of microstate analysis can be divided into four steps. In the first step, the EEG signals were bandpass (2-20Hz) filtered firstly and then the Global Field Power (GFP, defined as Equation (1)) was calculated for each time point [39]. In the second step, the EEG topographies corresponding to the maxima of GFP were submitted to the clustering algorithm considering that EEG signals at the time point of GFP maxima have a relatively high Signal/Noise ratio. The polarity of each topography was ignored. For each subject and each task condition, these procedures were repeated varying the number of clusters from 3 to 12. The Global Explain Variance (GEV) and the Cross-Validation (CV) criterion were used to determine the best number of microstates (defined as Equation (2) and (3)). These procedures were applied to the EEG of each subject and thus leaded to individual microstate classes. In the third step, the group-level microstate classes were obtained by a second clustering procedure in which the topographies of microstates of each subject were used as the clustering samples after the subject-level microstate analysis. At last, EEG topographies at each time point were allocated to one of the mean microstate classes by finding the maximum spatial correlation coefficient between the topography of each time point and the group-level mean microstate maps. The procedure of microstate analysis can be seen in the middle part of Fig. 1.

$$GFP = \sqrt{\left(\sum_{i}^{N} \left(V_i\left(t\right) - V_{mean}\left(t\right)\right)^2\right) \Big/ N_e} \tag{1}$$

where $V_i\left(t\right)$ and $V_{mean}\left(t\right)$ is the instantaneous and mean potentials across the N_e electrodes at time t.

$$GEV = \frac{\sum_{t=1}^{t\,\max} \left(GFP_u\left(t\right) \cdot C_{u,T_t}\right)^2}{\sum_{t=1}^{t\,\max} GFP_u^2\left(t\right)} \tag{2}$$

in which, $GFP_u\left(t\right)$ is the GFP of the data for Microstate U at time point t, T_t is the template map of Microstate U obtained by the analysis procedure, C_{u,T_t} is the spatial correlation between data of Microstate U at time point t and the template map T_t.

$$CV = \frac{\sum_{t=1}^{t\,\max} \left(\left\|u\left(t\right)\right\|^2 - T_t \cdot u\left(t\right)^2\right)}{t_{\max} \cdot \left(N_e - 1\right)} \cdot \left(\frac{N_e - 1}{N_e - 1 - q}\right)^2 \tag{3}$$

where q is the number of microstates.

Topographic analysis of variance (TANOVA) was implemented to evaluate the differences of each microstate class in each task [40]. To quantify the dynamic properties of microstates in each task condition, the following parameters were calculated: (1) Occurrence, defined as the number of a given microstate per second, (2) Duration, defined as the mean duration time of a microstate and (3) Coverage, calculated as the proportion of a given microstate.

E. Functional Connectivity Analysis

The pre-processed EEG data in section II.C were filtered into Theta and Alpha bands through an FIR bandpass filter. By calculating the Phase-locking value (PLV) between signal at different channels, two time-varying functional connectivity networks were constructed [41]. The PLV describes the phase synchronization of two EEG signals and ranges from 0 to 1, which was defined as:

$$PLV\left(t\right) = \frac{1}{N_{trial}} \left| \sum_{k=1}^{N} e^{i\left(\varphi_{(t,k)} - \psi_{(t,k)}\right)} \right| \tag{4}$$

where N_{trial} represents the trial number, $\varphi_{(t,k)}$ and $\psi\left(t,k\right)$ are the instant phase of EEG signal of channel φ and ψ at time point t, which was obtained by the Hilbert transform of the signal. After all the above, mean functional connectivity of each microstate was calculated by averaging the brain networks at time points that with same microstate labels.

The topological properties (i.e., the functional integration and segregation among different brain regions) can be quantified by using graph theory-based analysis [42]. Nodal and global metrics of the functional connectivity network at Theta and Alpha band in each microstate of each task were calculated by using the GRETNA toolbox [43]. The details are as follows.

1) Nodal Metrics: Degree of node i (k_i) is the number of nodes it directly connected, which was defined as:

$$k_i = \sum_{j \in N} a_{ij} \tag{5}$$

in which the a_{ij} is the connection strength between node i and j, N represents the node set of the network. Change of node degree reflects the change of the importance of this node in the network. Nodes whose degree changed with mental workload significantly were regarded as "core nodes" in this study.

2) Global Metrics: The global metrics can reflect the functional integration and segregation of a network. Characteristic Path Length (L_p) was defined as the average shortest path length between all pairs of nodes in the network, which reflected the global integration of the network. Shorter L_p means higher information transformation efficiency of a brain network. The L_p was defined as:

$$L_p = \frac{1}{N_e} \sum_{i \in N_{set}} L_i = \frac{1}{N_e} \sum_{i \in N_{set}} \frac{\sum_{j \in N_{set}, j \neq i} d_{ij}}{N_e - 1} \tag{6}$$

in which, L_i is the mean distance between node i and other nodes, d_{ij} is the shortest path length between node i and j, N_{set} refers to the set of all nodes.

Clustering coefficient (C_p) of node i is defined as the fraction of triangles around the node, the mean clustering coefficient of a network is the average C_p of all the nodes in the network. Larger mean C_p reflects higher local information processing of a network. Mean C_p was calculated as:

$$C_p = \frac{1}{N_e} \sum_{i \in N_{set}} C_i = \frac{1}{n} \sum_{i \in N_{set}} \frac{2t_i}{k_i\left(k_i - 1\right)} \tag{7}$$

Global efficiency (E_g) is another metric to describe the ability to transfer information between nodes. Unlike L_p, which is primarily influenced by long paths, E_g is primarily influenced by short paths hence making it a superior measure of integration. A network with higher E_g means faster

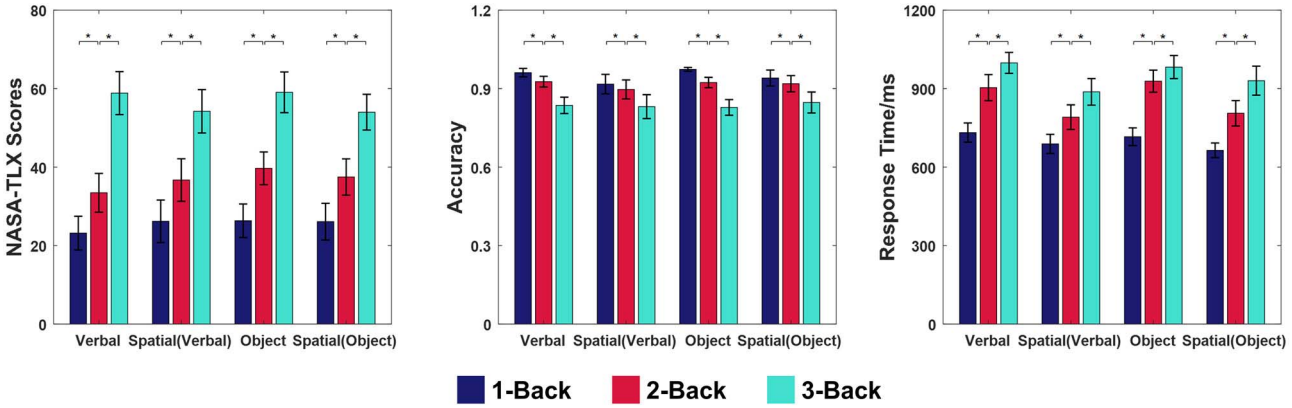

Fig. 3. Average behavioral results for each task condition for all participants (Annotations $*$ means $p < 0.05$).

information transferring speed between brain regions. The calculation of E_g was as follows:

$$E_g = \frac{1}{N_e}\sum_{i\in N_{set}} E_i = \frac{1}{N_e}\sum_{i\in N_{set}} \frac{\sum_{j\in N_{set}, j\neq i} d_{ij}^{-1}}{N_e - 1} \quad (8)$$

F. Statistical Analysis

Two-way repeated-measures ANOVA (RANOVA, Task load $\times$ Task type) was applied to test the effects of mental workload and information types on behavior metrics and the rationality of the experiment. To explore the correlations between microstate metrics and mental workload, Pearson correlation coefficient between microstate metrics and mean response time under different task conditions were calculated after the analysis of RANOVA. RANOVA was also applied on the brain network metrics of different frequencies and microstates for all the tasks subsequently to get nodal and global metrics that were significantly influenced by task load. Post hoc paired test were carried out on the selected network metrics and the significance level was set as $p < 0.05$ after Bonferroni correction. All the statistical analyses were carried out by using IBM SPSS 22.0.

G. Classification

To further validate the effectiveness of the proposed method and the selected microstate-functional-connectivity features in discriminating mental workload, a 3-class classification procedure for within-task and cross-task classification were performed by employing a SVM classifier. Specifically, nodal metrics, global metrics, and connectivity strength values that changed significantly with mental workload were used as the feature set. For within-task workload classification, a leave-one-subject-out cross validation procedure (i.e., trained on data from 15 of the participants and tested on the left one) was adopted for each of the four tasks; and for cross-task classification, data from three tasks were used as the training set and the left one as testing set, which can also be called as "leave-one-task-out cross validation" procedure. Classification accuracy, sensitivity and specificity were then evaluated.

III. Results

A. Behavioral Results

NASA-TLX Scores, Accuracy and Mean Response Time of different tasks were shown in Fig. 3. As expected, subjective scores in the four tasks increased with the task loads, whereas the accuracy decreased and the response time became longer significantly. RANOVA results revealed a main effect of task load on NASA-TLX scores ($p < 0.05$). Multiple comparisons showed that scores of tasks with different loads were significantly different from each other (1-Back vs. 2-Back: $p < 0.01$, 2-Back vs. 3-Back: ($p < 0.01$) in all four tasks. There's no main effect of task type on NASA-TLX scores ($p > 0.05$) and the interaction of the two factors was not significant ($p > 0.05$).

Consistent with NASA-TLX, significant differences in accuracy were found between different task loads, and no main effect has been found on task type and the interaction. Considering the mean response time, significant differences were found between different task loads ($p < 0.01$), and between different task types ($p < 0.01$). The interaction effect of these two factors was not significant ($p > 0.05$).

B. Microstate Dynamics

As shown in Fig. 4, six microstates labeled as MS A-F were determined according to the cross-validation criteria, which is highly consistent with the results of Custo [44]. In detail, the topographies of the six microstates are as follows: MS A had a left occipital to right frontal orientation, MS B was from right occipital to left frontal, MS C had a symmetric frontocentral to occipital regions, MS D was also symmetric, but with an occipital to prefrontal orientation, MS E had a right parietal to the superior temporal orientation, while the MS F originated from the right parietal to the left temporal. The GEV of these microstates in different tasks are as follows: Verbal task (1-Back: 65.75 $\pm$ 1.39%, 2-Back: 65.86 $\pm$ 1.69%, 3-Back: 66.19 $\pm$ 1.69%), Object task (1-Back: 65.38 $\pm$ 1.50%, 2-Back: 66.49 $\pm$ 1.56%, 3-Back: 66.14 $\pm$ 1.72%), Spatial (Verbal) task (1-Back: 65.35 $\pm$ 1.76%, 2-Back: 64.49 $\pm$ 1.99%, 3-Back: 64.65 $\pm$ 1.77%), Spatial (Object) task (1-Back: 65.15 $\pm$ 1.68%, 2-Back: 64.40 $\pm$ 1.75%, 3-Back:

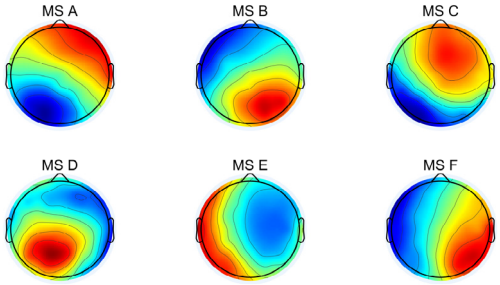

Fig. 4. Topographies of the six global microstates classes across task types, task loads and participants.

TABLE I
CORRELATION BETWEEN MICROSTATE METRICS AND RESPONSE TIME

		MS A	MS B	MS C	MS D	MS E	MS F
Occurrence	V	**-0.552****	-0.156	**-0.327***	0.260	**-0.415****	**-0.387****
	O	-0.125	0.200	**-0.327***	**0.339***	-0.011	-0.013
	S(V)	**-0.379****	-0.106	**-0.394****	-0.037	**-0.334***	0.026
	S(O)	0.029	-0.006	0.154	-0.072	-0.243	0.059
Duration	V	**-0.496****	-0.222	-0.110	0.085	-0.270	**-0.306***
	O	0.043	-0.068	-0.246	0.159	-0.130	0.026
	S(V)	**-0.293***	0.107	-0.185	0.006	-0.160	0.028
	S(O)	-0.006	0.078	0.205	-0.056	-0.089	-0.006
Coverage	V	**-0.502****	-0.142	-0.249	0.244	**-0.363***	**-0.332***
	O	-0.123	0.135	**-0.363***	**0.296***	-0.055	0.015
	S(V)	**-0.343***	-0.038	**-0.329***	-0.036	**-0.322***	0.020
	S(O)	0.020	0.066	0.188	-0.045	-0.215	0.060

Note: V=Verbal, O=Object, S(V)=Spatial (Verbal), S(O)=Spatial (Object). * p<0.05, ** p<0.01.

65.33 ± 1.84%). Results of TANOVA showed that there's no difference of microstate among different tasks.

Statistical analyses on microstate metrics showed that Occurrence of all the microstates except MS E, the Duration of MS A and MS C, as well as the Coverage of MS A, MS C, and MS F were significantly affected by task loads ($p < 0.05$). Significant effects of task type on all these metrics were observed ($p < 0.05$). To further explore the relationship between microstate metrics and mental workload in the four tasks, Pearson correlation coefficient between the microstate metrics and the mean response time of participants were carried out, which can be seen in Table I. It can be known from Table I that all the metrics of MS A, Occurrence and Coverage of MS E in Verbal and Spatial (Verbal) tasks, and all the metrics of MS F in Verbal tasks showed a negative correlation with the mean response time significantly. Occurrence and Coverage of MS C also showed a negative correlation with the mean response time in all tasks except the Spatial (Object) task. Occurrence and Coverage of MS D in Object task was positively correlated with mean response time.

C. Nodal Properties

Fig. 5 (A) showed the distribution of core nodes in different microstates in the four tasks respectively. It can be seen that 91.14% (average of Theta and Alpha bands) of the core nodes were found in MS C, MS D, and MS F (specifically, MS C: 26.58%, MS D: 24.05%, MS F:40.51%) in Verbal task, and 90.68% of the core nodes were found in MS B, MS C, MS D, and MS F (specifically, MS B: 31.06%, MS C: 16.15%, MS D: 27.33%, MS F:16.15%) in Spatial (Verbal) task. The core nodes in Object and Spatial (Object) tasks showed an even distribution in the 6 microstates.

The distribution of core nodes in different brain regions in the four tasks was shown in Fig. 5 (B). It was found that about 90% (average of Theta and Alpha bands) of nodes existed in the Frontal, Central, and Parietal Cortex in all four tasks. Specifically, in Verbal task, number of core nodes in Frontal accounts for 44.04% and Central 28.03%, Parietal 20.67%, respectively; in Object task, Frontal 27.08%, Central 33.39%, Parietal 30.55%; in Spatial (Verbal) task, Frontal 23.26%, Central 37.02%, Parietal 32.30%, and in Spatial (Object) task, Frontal 28.13%, Central 30.48%, Parietal 30.90%. In all these nodes, the degrees of node FC6 from MS C, node FPz, F1, FC3, FC1, P4 from MS D, node Fz, F2, FCz and FC2 from MS F in Theta band brain network as well as node Fz, FC1 from MS D, node Fz, F2, FCz from MS F in Alpha band brain network (totally 15 core nodes) were significantly affected by task loads in all the four tasks. Mean distribution in Microstates and Brain Regions (across the four tasks) were presented in Fig. 5 (C).

D. Connectivity Strength

In a similar way, connectivity that varied significantly with mental workload in each task were obtained firstly, then the connectivity that affected by mental workload in all the four tasks were selected, which resulted in 68 pairs of connectivity mainly distributed in MS B, MS C and MS D (Fig. 6, MS B: 29 pairs, MS C: 20 pairs and MS D: 16 pairs respectively) in total. Specifically, connectivity in MS B was mainly located in the Frontal area (account for 41.38%) and the Frontal-Parietal area (account for 27.59%); connectivity in MS C were mainly located in the Frontal-Central (account for 50%) and Parietal area (account for 45%); connectivity in MS D mainly located in the Frontal-Parietal area (account for 68.75%); connectivity in MS E and MS F located in the Frontal-Central area.

E. Global Properties

Fig. 7 showed the characteristic path length, mean clustering coefficient, and global efficiency of brain networks with different frequency bands and different microstates in the four tasks. RANOVA showed that with the increment of task load, the characteristic path length of MS D network in both Theta and Alpha bands decreased significantly, whereas the mean clustering coefficient of MS C and MS D network in both frequency bands, as well as the global efficiency of MS C network in Alpha band and MS D network in both frequency bands increased significantly. There's no significant effect of task type on all the metrics mentioned above ($p > 0.05$).

To further explore the changes of global metrics of functional connectivity networks with mental workload, One-way ANOVA (Factor: task load) was utilized in each task. Post hoc test results showed that in all the four tasks, the MS D network in both frequency bands tended to have shorter characteristic path length and higher global efficiency when the task load increased. It should be noticed that in the Object task, with the increment of mental workload, the Cp decreased firstly

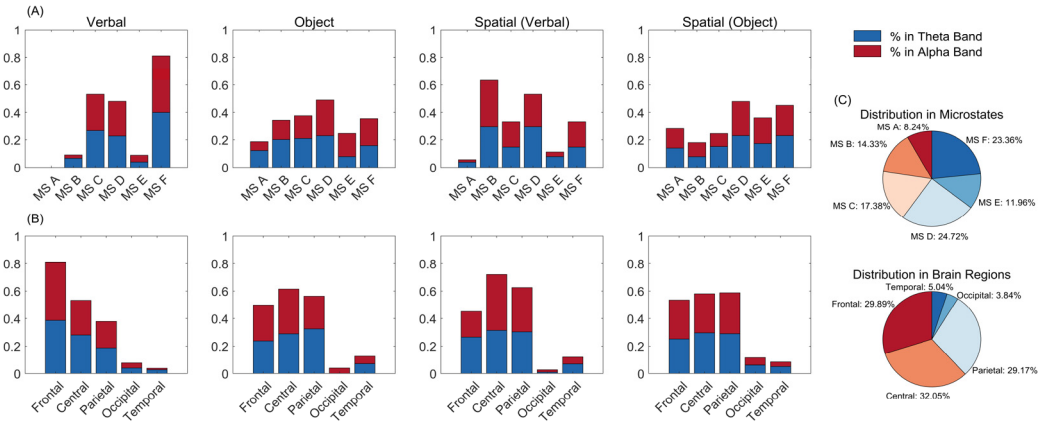

Fig. 5. Core nodes distributions in microstates and brain regions.

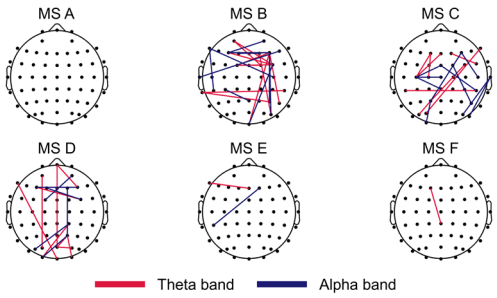

Fig. 6. Connectivity with significant effects of task load in all the tasks.

and then increased slightly, and the Eg increased firstly and then decreased slightly, whereas there's no difference between 2-Back and 3-Back condition (1-Back vs. 2-Back: $p < 0.05$, 1-Back vs. 3-Back: $p < 0.05$, 2-Back vs. 3-Back: $p > 0.05$).

F. Classification Performance

Nodal metrics, global metrics and the connectivity strength that varied significantly with mental workload in all the four tasks were used in the classification, which included degree of 15 core nodes, 68 connectivity strength and 9 global metrics. Table II showed the classification performance of these features in discriminating mental workload both in within-task and cross-task scenario. In detail, an averaged 95.8% accuracy for within-task classification and 80.3% for cross-task classification were achieved. The comparison of the proposed method with state-of-the-art methods was shown in Table III.

IV. Discussion

The accurate evaluation of cross-task mental workload based on physiological signals such as EEG remains unsolved. Change of dynamic functional connectivity properties with mental workload in different tasks were explored by designing mental workload tasks of different information types and using a dynamic functional connectivity analysis method based on EEG microstate analysis in this paper. Behavior results showed that the experiments designed in this paper can evoke

TABLE II
WITHIN AND CROSS TASK CLASSIFICATION PERFORMANCE OF THE PROPOSED METHOD

	Train on	Test on	Accuracy	Sensitivity	Specificity
Within task	V	V	0.943±0.036	0.943±0.037	0.971±0.018
	O	O	0.960±0.035	0.959±0.034	0.981±0.016
	S(V)	S(V)	0.960±0.036	0.958±0.037	0.980±0.018
	S(O)	S(O)	0.970±0.018	0.969±0.019	0.985±0.010
	Average		0.958	0.957	0.979
Cross task	V	Others	0.798±0.068	0.793±0.059	0.897±0.030
	O	Others	0.799±0.045	0.789±0.048	0.899±0.023
	S(V)	Others	0.833±0.055	0.823±0.058	0.915±0.027
	S(O)	Others	0.782±0.085	0.779±0.086	0.890±0.044
	Average		0.803	0.796	0.900

Note: V: Verbal, O: Object, S(V): Spatial (Verbal), S(O): Spatial (Object).

different mental workload levels of participants effectively. Six microstates were determined to describe the EEG activities under tasks according to the CV criteria, which was highly consistent with that of Custo's [44]. Results showed that the microstate parameters were significantly affected by mental workload levels, however the types of information to be dealt with had a greater impact on the microstate parameters, i.e., variation of microstate parameters with mental workload in different tasks differs from each other. Analysis of nodal metrics of brain network under different microstates showed that the degree of nodes and connectivity strength in Frontal-Parietal network changed significantly with mental workload. Among these, the degree of 15 nodes and strength of 68 pairs of connectivity changed with mental workload in a consistent way in all four tasks, which may have the potential to be used in cross-task mental workload evaluation. Analysis of global metrics of brain network showed that with the increment of mental workload, characteristic path length of MS D decreased, whereas global efficiency of MS D increased significantly in all the four tasks, which may reflect that the information transfer efficiency was strengthened in the cognitive control network of brain while dealing with high mental workload tasks. Further, the effectiveness of the proposed method and selected features in discriminating mental workload was validated by using a SVM classifier,

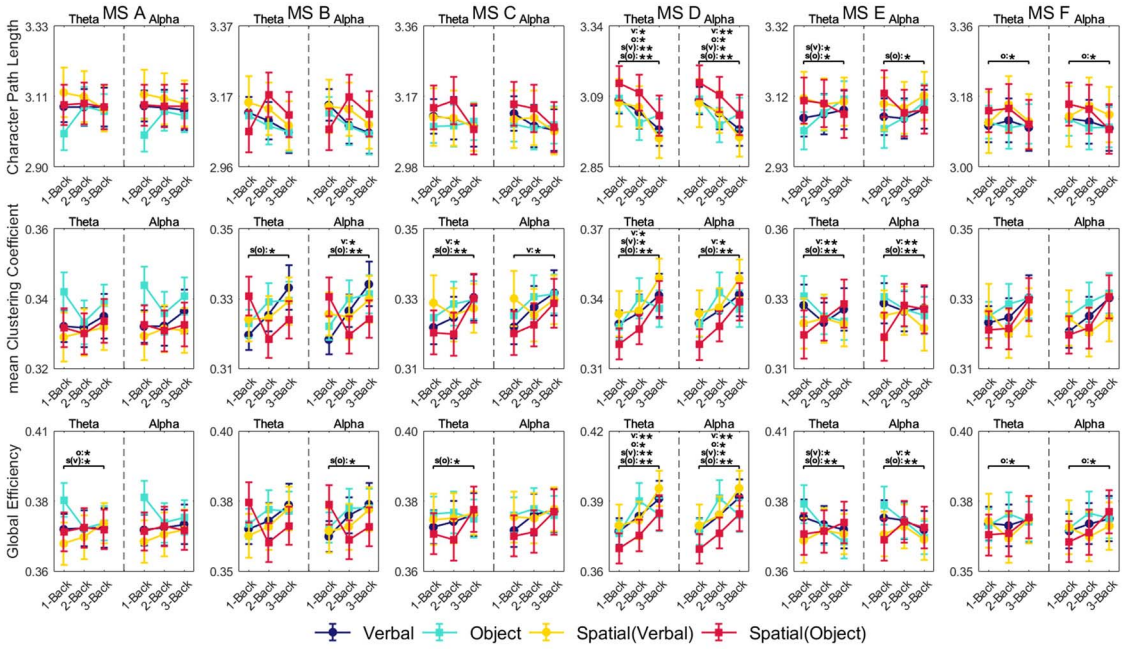

Fig. 7. Global metrics of functional connectivity networks with different microstates and frequency bands in each task (* means $p < 0.05$ and ** means $p < 0.01$).

TABLE III
COMPARISON BETWEEN THE PROPOSED METHOD AND STATE-OF-THE-ART STUDIES

	Features	Methods	Tasks	Classes	Accuracy
Baldwin [9]	PSD	ANN	Reading span, Spatial N-Back, Sternberg tasks	Binary	0.450
Walter [10]	ERS/ERD	SVM	GO/NO-GO, Verbal N-Back, Reading span, Algebra problem task	Binary	0.540
Ke [11]	PSD	SVM	Verbal N-Back, Spatial N-Back	4-class	0.290
Dimitrakopoulos [50]	Cortical connectivity	SVM	Verbal N-Back, Arithmetic tasks	Binary	0.870
Zhang [16]	Spatial-spectral-temporal	R3DCNN	Spatial N-Back, Arithmetic tasks	Binary	0.889
The proposed method	Microstate-functional connectivity	SVM	Verbal, Object, Spatial (Verbal), Spatial (Object) N-Back tasks	3-class	0.803

an average accuracy of 95.8% for within-task and 80.3% for cross-task workload classification were achieved. These results may provide theoretical basis and practical references in the accurate evaluation of cross-task mental workload.

A. Microstate Dynamic

Researches on neuroimaging have related the EEG microstates with specific cognitive functions. This is because different topographic maps of microstates are generated by activation of different brain regions that are responsible for specific cognitive functions [32], [44]. MS A was thought to be associated with the phonological loop of brain, which was in charge of the storage and control of verbal information in the working memory model raised by Baddeley [45]. The phenomenon that parameters of MS A decreased significantly when workload raised in Verbal task may reflect that the phonological loop of brain was dominated by the memory load when dealing with verbal information. It should be noticed that the parameters of MS A decreased significantly with workload in Spatial (Verbal) task, in which the verbal information was not set as target stimuli though. In other words, the distracting stimulation of verbal information had attracted the attention of participants [46]. The dynamics of MS C reflected the aspects of attention, focus switching, and reorientation of the dorsal attention network of brain [47], [48]. In this study, the Coverage and Occurrence of MS C decreased when workload increased in all tasks except Spatial (Object) task, which was a reflection of the brain's adjustment to the allocation of attention resources under different levels of task loads. MS D, which originated from the posterior cingulate cortex, is associated with the activities of the cognitive control network of brain and is in charge of the advanced cognitive activities of brain. It was found that the parameters of MS D tend to be larger when mental workload increased in the content-type (Verbal and Object) tasks, which reflected the change of activation level of the cognitive control network of brain when dealing with different intensities of information flow. These results are consistent with the research of Milz [48] that compared with the rest state, the parameters of MS C decreased whereas that of MS D increased under cognitive tasks. Custo [44] found that MS E mainly initiated from the cerebellum region and was believed to associate with the sensorimotor function of brain. The parameters of MS E in all the four tasks decreased when the mental workload increased (although the significant effect was found only in Verbal and Spatial (Verbal) tasks), which may reflect the

process of motion preparation after information memorizing and processing of brain. MS F, which originated from the anterior cingulate cortex, was considered as the default mode network of brain [44]. The dynamics of MS F were thought to be associated with the cognitive processing evoked by task demands, whereas changes of MS F parameters were found only in the Verbal task.

Results showed that the variation of microstate parameters with mental workload in different tasks differs from each other greatly. On the one hand, these results implied that different cognitive functional networks were involved when the brain was dealing with different information. On the other hand, it can be inferred that the mental workload levels cannot be effectively described by the microstate parameters and therefore it's not applicable in cross-task mental workload evaluation.

B. Functional Connectivity

The change of node degree can describe the participation of the node in information transferring in a network when performing tasks, and the connectivity strength between nodes was a reflection of information transfer efficiency within a specific brain region or between different brain regions. The distribution of nodes and connectivity that were significantly affected by the mental workload in different microstates and brain regions were analyzed in this study. Results showed that nodes whose degree changed with mental workload significantly (namely core nodes) were mainly distributed in MS C, MS D and MS F (shown in Fig. 5), which reflected that the attention network, the cognitive control network and the default mode network were adjusted by the mental workload in tasks with different information types [48]. The brain tended to allocate more attention resources and change the efficiency of information transfer in the cognitive control network to deal with the pressure of higher information flow intensity. It should be noticed that the connectivity strength between nodes in the Frontal-Parietal regions of MS B network changed significantly with mental workload in the four tasks though the dynamic properties of MS B were not affected by mental workload (Fig. 6). Considering the close association of MS B with the visual system of brain, it may reflect the adjustment of information flow intensity on the brain's visual system.

Although the distribution of nodes whose degree was affected by the mental workload differs in microstates, more than 90% of these nodes existed in the Frontal-Parietal regions. Among these nodes, the degree of 15 nodes changed significantly with task loads in all four tasks. In the same way, 68 pairs of connectivity changed significantly with task loads in all four tasks. All the 15 nodes and the 68 pairs of connectivity distributed in the Frontal-Parietal region, which was consistent with the conclusion that the Frontal-Parietal region of brain was involved in the process of working memory [21], [49], [50]. Mencarelli [49] thought that the dorsolateral prefrontal cortex (DLPFC) was involved in the short-term storage and processing of information, and these processes had nothing to do with the type of information. However, more evidence from neuroimaging researches is needed to prove these theories. Furtherly, considering that the working memory process includes several periods (i.e., encoding, maintaining, retrieval and action periods) [5], [8], clarifying which period was influenced by mental workload the most might provide reliable references to the accurate evaluation of mental workload. Despite these, the change of connectivity strength in Frontal-Parietal regions of brain reflected the increment or decrement of synergy between these brain regions when dealing with tasks of different mental workloads. These results may provide a valuable reference to the accurate evaluation of cross-task mental workload.

Various researches indicated that the functional integration of brain network tended to be strengthened to deal with the pressure of higher information flow intensity when the mental workload increased [21], [51]. This regularity was found in the MS D network in both Theta and Alpha band in this study (Fig. 7). Specifically, the brain network of both frequency bands in the cognitive control network tended to have shorter characteristic path length and higher global efficiency under high mental workload tasks, which reflected that the interaction between different brain regions was strengthened and the efficiency of information transfer of the whole network was promoted in the cognitive control network when the mental workload increased [21]–[22], [51].The slight difference between 2-Back and 3-Back in the Object task may be attributed to the constraint of working memory that the response of human brain approached a plateau when task load met or exceeded the capacity [26]. However, more experiments and investigations should be carried out to validate this hypothesis. Method that can accurately quantify the amount of information needs to be developed too. Even though, these results indicated that these metrics have the potential to be applied in the cross-task mental workload evaluation.

In conclusion, several meaningful results were obtained after analyzing the changes of functional connectivity properties with mental workload in cognitive tasks of different information types, including: (1) Six microstate topographies were obtained to describe the brain dynamics under tasks, which were highly consistent with previous studies; (2) The microstate parameters were significantly affected by mental workload levels, however the types of information to be dealt with had greater impact on the microstate parameters, i.e., variation of microstate parameters with mental workload in different tasks differs from each other; (3) In the functional connectivity network under different microstates, 15 nodes and 68 pairs of connectivity from the Frontal-Parietal region were found to be sensitive to mental workload in all four tasks, which indicated that these node metrics have potential to effectively evaluate mental workload in cross-task scenario; (4) In all the four tasks, characteristic path length of MS D decreased whereas the global efficiency increased when the mental workload tended to be high, which implied that the interaction between different brain regions was strengthened and the efficiency of information transfer of the whole network was enhanced; (5) By using a SVM classifier, an averaged accuracy of 95.8% for within-task and 80.3% for cross-task workload classification were achieved. These results can provide a theoretical basis for the accurate evaluation of cross-task

mental workload. Despite all these above, this research is still limited to a pre-set task environment: all the four tasks were designed by using the N-Back paradigm with the same form but different types of information. However, in real human-machine interaction tasks, the operators often face more complex information types or need to complete more complicated information processing. Therefore, the effectiveness of the proposed metrics needs to be further verified when it is applied to real scenarios.

ACKNOWLEDGMENT

The authors would like to thank all of the participants who generously volunteered their time to participate in this study.

REFERENCES

[1] J. Paxion, E. Galy, and C. Berthelon, "Mental workload and driving," *Frontiers Psychol.*, vol. 5, p. 1344, Dec. 2014.

[2] J. Heard, C. E. Harriott, and J. A. Adams, "A survey of workload assessment algorithms," *IEEE Trans. Human-Mach. Syst.*, vol. 48, no. 5, pp. 434–451, Oct. 2018.

[3] K. J. Jaquess *et al.*, "Changes in mental workload and motor performance throughout multiple practice sessions under various levels of task difficulty," *Neuroscience*, vol. 393, pp. 305–318, Nov. 2018.

[4] S. G. Hart and L. E. Staveland, "Development of NASA-TLX (Task Load Index): Results of empirical and theoretical research," *Adv. Psychol.*, vol. 52, pp. 139–183, Apr. 1988.

[5] E. Astrand, "A continuous time-resolved measure decoded from EEG oscillatory activity predicts working memory task performance," *J. Neural Eng.*, vol. 15, no. 3, Apr. 2018, Art. no. 036021.

[6] M. A. Hogervorst, A.-M. Brouwer, and J. B. F. van Erp, "Combining and comparing EEG, peripheral physiology and eye-related measures for the assessment of mental workload," *Frontiers Neurosci.*, vol. 8, p. 322, Oct. 2014.

[7] P. Zhang, X. Wang, J. Chen, and W. You, "Feature weight driven interactive mutual information modeling for heterogeneous bio-signal fusion to estimate mental workload," *Sensors*, vol. 17, no. 10, p. 2315, Oct. 2017.

[8] W. J. Chai, A. I. Abd Hamid, and J. M. Abdullah, "Working memory from the psychological and neurosciences perspectives: A review," *Frontiers Psychol.*, vol. 9, p. 401, Mar. 2018.

[9] C. L. Baldwin and B. N. Penaranda, "Adaptive training using an artificial neural network and EEG metrics for within- and cross-task workload classification," *NeuroImage*, vol. 59, no. 1, pp. 48–56, Jan. 2012.

[10] C. Walter, S. Schmidt, W. Rosenstiel, P. Gerjets, and M. Bogdan, "Using cross-task classification for classifying workload levels in complex learning tasks," in *Proc. Humaine Assoc. Conf. Affect. Comput. Intell. Interact.*, Sep. 2013, pp. 876–881.

[11] Y. Ke *et al.*, "An EEG-based mental workload estimator trained on working memory task can work well under simulated multi-attribute task," *Frontiers Hum. Neurosci.*, vol. 8, p. 703, Sep. 2014.

[12] T. B. Christophel, P. C. Klink, B. Spitzer, P. R. Roelfsema, and J.-D. Haynes, "The distributed nature of working memory," *Trends Cognit. Sci.*, vol. 21, no. 2, pp. 111–124, Feb. 2017.

[13] H. Walter *et al.*, "Evidence for quantitative domain dominance for verbal and spatial working memory in frontal and parietal cortex," *Cortex*, vol. 39, nos. 4–5, pp. 897–911, 2003.

[14] J. Pan *et al.*, "Prognosis for patients with cognitive motor dissociation identified by brain-computer interface," *Brain*, vol. 143, no. 4, pp. 1177–1189, Apr. 2020.

[15] J. Jin, R. Xiao, I. Daly, Y. Miao, X. Wang, and A. Cichocki, "Internal feature selection method of CSP based on L1-norm and Dempster–Shafer theory," *IEEE Trans. Neural Netw. Learn. Syst.*, vol. 32, no. 11, pp. 4814–4825, Nov. 2021.

[16] P. Zhang, X. Wang, W. Zhang, and J. Chen, "Learning spatial–spectral–temporal EEG features with recurrent 3D convolutional neural networks for cross-task mental workload assessment," *IEEE Trans. Neural Syst. Rehabil. Eng.*, vol. 27, no. 1, pp. 31–42, Jan. 2019.

[17] A. Gevins, M. E. Smith, L. McEvoy, and D. Yu, "High-resolution EEG mapping of cortical activation related to working memory: Effects of task difficulty, type of processing, and practice," *Cerebral Cortex*, vol. 7, no. 4, pp. 374–385, Jun. 1997.

[18] T. Popov, P. Popova, M. Harkotte, B. Awiszus, B. Rockstroh, and G. A. Miller, "Cross-frequency interactions between frontal theta and posterior alpha control mechanisms foster working memory," *NeuroImage*, vol. 181, pp. 728–733, Nov. 2018.

[19] F. Dehais *et al.*, "Monitoring pilot's mental workload using ERPs and spectral power with a six-dry-electrode EEG system in real flight conditions," *Sensors*, vol. 19, no. 6, p. 1324, Mar. 2019.

[20] A.-M. Brouwer, M. A. Hogervorst, J. B. F. van Erp, T. Heffelaar, P. H. Zimmerman, and R. Oostenveld, "Estimating workload using EEG spectral power and ERPs in the n-back task," *J. Neural Eng.*, vol. 9, no. 4, Aug. 2012, Art. no. 045008.

[21] Z. Dai *et al.*, "EEG cortical connectivity analysis of working memory reveals topological reorganization in theta and alpha bands," *Frontiers Human Neurosci.*, vol. 11, p. 237, May 2017.

[22] F. Taya, Y. Sun, F. Babiloni, N. V. Thakor, and A. Bezerianos, "Topological changes in the brain network induced by the training on a piloting task: An EEG-based functional connectome approach," *IEEE Trans. Neural Syst. Rehabil. Eng.*, vol. 26, no. 2, pp. 263–271, Feb. 2018.

[23] J. Jin, Z. Wang, R. Xu, C. Liu, X. Wang, and A. Cichocki, "Robust similarity measurement based on a novel time filter for SSVEPs detection," *IEEE Trans. Neural Netw. Learn. Syst.*, early access, Oct. 14, 2021, doi: 10.1109/TNNLS.2021.3118468.

[24] M. Rubinov and O. Sporns, "Complex network measures of brain connectivity: Uses and interpretations," *NeuroImage*, vol. 52, no. 3, pp. 1059–1069, Apr. 2010.

[25] L. E. Ismail and W. Karwowski, "A graph theory-based modeling of functional brain connectivity based on EEG: A systematic review in the context of neuroergonomics," *IEEE Access*, vol. 8, pp. 155103–155135, 2020.

[26] D. Zhang, H. Zhao, W. Bai, and X. Tian, "Functional connectivity among multi-channel EEGs when working memory load reaches the capacity," *Brain Res.*, vol. 1631, pp. 101–112, Jan. 2016.

[27] R. M. Hutchison *et al.*, "Dynamic functional connectivity: Promise, issues, and interpretations," *Neuroimage*, vol. 80, pp. 360–378, Oct. 2013.

[28] P. Zhang, X. Wang, J. Chen, W. You, and W. Zhang, "Spectral and temporal feature learning with two-stream neural networks for mental workload assessment," *IEEE Trans. Neural Syst. Rehabil. Eng.*, vol. 27, no. 6, pp. 1149–1159, Jun. 2019.

[29] S. Ren, J. Li, F. Taya, J. deSouza, N. V. Thakor, and A. Bezerianos, "Dynamic functional segregation and integration in human brain network during complex tasks," *IEEE Trans. Neural Syst. Rehabil. Eng.*, vol. 25, no. 6, pp. 547–556, Jun. 2017.

[30] G. C. O'Neill, P. Tewarie, D. Vidaurre, L. Liuzzi, M. W. Woolrich, and M. J. Brookes, "Dynamics of large-scale electrophysiological networks: A technical review," *NeuroImage*, vol. 180, pp. 559–576, Oct. 2018.

[31] D. Lehmann, W. K. Strik, B. Henggeler, T. Koenig, and M. Koukkou, "Brain electric microstates and momentary conscious mind states as building blocks of spontaneous thinking: I. Visual imagery and abstract thoughts," *Int. J. Psychophysiol.*, vol. 29, no. 1, pp. 1–11, Jun. 1998.

[32] C. M. Michel and T. Koenig, "EEG microstates as a tool for studying the temporal dynamics of whole-brain neuronal networks: A review," *NeuroImage*, vol. 180, pp. 577–593, Oct. 2018.

[33] D. Lehmann, H. Ozaki, and I. Pal, "EEG alpha map series: Brain micro-states by space-oriented adaptive segmentation," *Electroencephalogr. Clin. Neurophysiol.*, vol. 67, no. 3, pp. 271–288, Sep. 1987.

[34] C. S. Deolindo *et al.*, "Microstates in complex and dynamical environments: Unraveling situational awareness in critical helicopter landing maneuvers," *Hum. Brain Mapping*, vol. 42, no. 10, pp. 3168–3181, Jul. 2021.

[35] M. Krylova *et al.*, "Evidence for modulation of EEG microstate sequence by vigilance level," *NeuroImage*, vol. 224, Jan. 2021, Art. no. 117393.

[36] M. Chaumon, D. V. M. Bishop, and N. A. Busch, "A practical guide to the selection of independent components of the electroencephalogram for artifact correction," *J. Neurosci. Methods*, vol. 250, pp. 47–63, Jul. 2015.

[37] A. Khanna, A. Pascual-Leone, and F. Farzan, "Reliability of resting-state microstate features in electroencephalography," *PLoS One*, vol. 9, no. 12, Dec. 2014, Art. no. e114163.

[38] M. M. Murray, D. Brunet, and C. M. Michel, "Topographic ERP analyses: A step-by-step tutorial review," *Brain Topogr.*, vol. 20, no. 4, pp. 249–264, Jun. 2008.
[39] T. Koenig *et al.*, "Millisecond by millisecond, year by year: Normative EEG microstates and developmental stages," *NeuroImage*, vol. 16, no. 1, pp. 41–48, May 2002.
[40] T. Koenig, M. Kottlow, M. Stein, and L. Melie-García, "Ragu: A free tool for the analysis of EEG and MEG event-related scalp field data using global randomization statistics," *Comput. Intell. Neurosci.*, vol. 2011, Feb. 2011, Art. no. e938925.
[41] J. P. Lachaux, E. Rodriguez, J. Martinerie, and F. J. Varela, "Measuring phase synchrony in brain signals," *Hum. Brain Mapping*, vol. 8, no. 4, pp. 194–208, Jan. 1999.
[42] B. He *et al.*, "Electrophysiological brain connectivity: Theory and implementation," *IEEE Trans. Biomed. Eng.*, vol. 66, no. 7, pp. 2115–2137, Jul. 2019.
[43] J. Wang, X. Wang, M. Xia, X. Liao, A. Evans, and Y. He, "GRETNA: A graph theoretical network analysis toolbox for imaging connectomics," *Frontiers Hum. Neurosci.*, vol. 9, p. 386, Jun. 2015.
[44] A. Custo, D. Van De Ville, W. M. Wells, M. I. Tomescu, D. Brunet, and C. M. Michel, "Electroencephalographic resting-state networks: Source localization of microstates," *Brain Connectivity*, vol. 7, no. 10, pp. 671–682, Dec. 2017.
[45] A. D. Baddeley, "Working memory," *Science*, vol. 255, no. 5044, pp. 556–559, Jan. 1992.
[46] N. Lavie, "Distracted and confused?: Selective attention under load," *Trends Cognit. Sci.*, vol. 9, no. 2, pp. 75–82, Feb. 2005.
[47] J. Britz, D. Van De Ville, and C. M. Michel, "BOLD correlates of EEG topography reveal rapid resting-state network dynamics," *NeuroImage*, vol. 52, no. 4, pp. 1162–1170, Oct. 2010.
[48] P. Milz, P. L. Faber, D. Lehmann, T. Koenig, K. Kochi, and R. D. Pascual-Marqui, "The functional significance of EEG microstates—Associations with modalities of thinking," *NeuroImage*, vol. 125, pp. 643–656, Jan. 2016.
[49] L. Mencarelli *et al.*, "Stimuli, presentation modality, and load-specific brain activity patterns during n-back task," *Hum. Brain Mapping*, vol. 40, no. 13, pp. 3810–3831, Sep. 2019.
[50] G. N. Dimitrakopoulos *et al.*, "Task-independent mental workload classification based upon common multiband EEG cortical connectivity," *IEEE Trans. Neural Syst. Rehabil. Eng.*, vol. 25, no. 11, pp. 1940–1949, Nov. 2017.
[51] I. Kakkos *et al.*, "Mental workload drives different reorganizations of functional cortical connectivity between 2D and 3D simulated flight experiments," *IEEE Trans. Neural Syst. Rehabil. Eng.*, vol. 27, no. 9, pp. 1704–1713, Sep. 2019.